Investigating Fiber Reinforcement Effects on the Performance of Concrete Pavements under Repeated Load

Mahmood Ghanim Abdul Jawad
Department of Civil Engineering, University of Baghdad, Baghdad, Iraq
mahmoud.gawad2201m@coeng.uobaghdad.edu.iq (corresponding author)

Amjad H. Khalil Albayati
Department of Civil Engineering, University of Baghdad, Baghdad, Iraq
a.khalil@uobaghdad.edu.iq

Received: 21 February 2025 | Revised: 28 March 2025 | Accepted: 2 April 2025

 DOI: https://doi.org/10.48084/etasr.10663

ABSTRACT

Concrete pavements are essential to modern infrastructure, but their low tensile and flexural strengths can cause cracking and shrinkage. This study evaluates fiber reinforcement with steel and carbon fibers in various combinations to improve rigid pavement performance. Six concrete mixes were tested: a control mix with no fiber, a mix with 1% steel fiber (SF1%), a mix with 1% carbon fiber (CF1%), and three hybrid mixes with 1% fiber content: 0.75% steel /0.25% carbon fiber (SF0.75CF0.25), 0.25% steel /0.75% carbon fiber (SF0.25CF0.75), and 0.5% steel /0.5% carbon fiber ((SF0.5CF0.5). Laboratory experiments including compressive, flexural, and splitting tensile strength tests were conducted at 7, 28, and 90 days, while Finite Element Analysis (FEA) using ABAQUS software was developed to examine pavement behavior under repeated loading. The results revealed that at 90 days, the SF1% mix exhibited a 9.1% improved compressive strength and CF1% mix a 7.3% improved strength over the control mix. The SF1% mix increased flexural strength by 72.5% and the CF1% mix by 48.6%. Additionally, splitting tensile strength increased by 70% for the SF1% and 45.5% for the CF1%. The hybrid mixes improved compressive strength by 7.6%-8.5%, flexural strength by 59.7%-70.2%, and splitting tensile strength by 56%-67.8%. The finite element modeling showed that the control mix was displaced 15 mm under repeated loading, while the SF1% reduced displacement by 35% and the hybrid mixes by 30%. These findings indicated that SF1% exhibited the best mechanical properties. However, fiber reinforcement, whether used single or in hybrid combinations, improves concrete pavement mechanical performance and loading behavior, offering a promising way to infrastructure durability and service life.

Keywords-concrete pavements; fiber reinforcement; mechanical properties; finite element analysis; ABAQUS

I. INTRODUCTION

Concrete pavements are essential to modern infrastructures, especially in roads, highways, airports, and industrial flooring due to their ability to withstand heavy traffic loads as well as severe environmental conditions. Conventional concrete, despite its excellent compressive strength, is naturally weak exhibiting limited tensile and flexural capacities [1]. These challenges make it sensitive to shrinkage, thermal cracking, fatigue cracking, and premature distress, leading to increased maintenance costs, structural weakening, and reduced service life [2-4].

To overcome these limitations, recent advancements in construction engineering have focused on fiber reinforcement as a promising strategy to enhance concrete performance. By incorporating fibers, such as steel and carbon into the concrete matrix, significant improvements in ductility, tensile strength, toughness, and flexural performance can be achieved. These fibers act as micro-crack arrestors, effectively delaying crack initiation and propagation, enhancing the mechanical performance of the mixture. Additionally, hybrid fiber systems that combine different types of fibers offer interactive benefits, further improving the overall performance of concrete under diverse and demanding conditions [5-7].

While laboratory studies have greatly expanded the understanding of Fiber-Reinforced Concrete (FRC), assessing its performance with complex, dynamic loads requires advanced numerical tools and computational techniques. In this study, numerical modeling, particularly FEA using ABAQUS software is utilized to simulate and analyze the behavior of various FRC mixes subjected to repeated loading conditions with real-world traffic simulations [8, 9]. The FEA, augmented by extensive experimental tests for the evaluation of compressive, tensile, and flexural strengths recorded at various

curing ages, will help improve the details of the examination and validation of displacement patterns, stress distributions, and fatigue properties. This methodological approach provides a deeper understanding of the underlying mechanisms through which fiber reinforcement significantly enhances pavement durability and mechanical performance [10, 11]. By combining rigorous experimental evaluation with advanced numerical simulation, this research establishes a robust framework for optimizing the mechanical performance and durability of concrete pavements, examining the possibility of FRC as a transformative material in modern pavement engineering.[12].

II. MATERALS

A. Cement

In this research, sulfate-resistant Portland cement (Type V) manufactured by the Iraqi Al-Mass Group was utilized. The chemical and physical properties of cement, as presented in Table I, meet the requirements specified in ASTM C150/C150M [13].

TABLE I. PHYSICOCHEMICAL PROPERTIES OF CEMENT

Physical porperties	**Results**	**ASTM C150/C150M**
Fineness (m²/kg)	360	≥ 280 m²/kg
Soundness (%)	0.045	≤ 0.80%
Initial setting time (min)	90	≥ 45 min
Final setting time (min)	420	≤ 600min
Compression strength-3 days (MPa)	29	≥ 10 MPa (3 days)
Compression strength-28 days (MPa)	42.8	≥ 28 MPa (28 days)
Chemical porperties	**Results**	**ASTM C150/C150M**
Lime	61.21%	-
Silica	23.7%	-
Alumina	5.58%	-
Iron Oxide	3.48%	-
Magnesia	2.27%	≤ 6.0%
Sulfate	2.10%	≤ 3.0%

B. Aggregates

Natural sand (fine aggregate) and crushed gravel (coarse aggregate), both consisting of quartz-based materials, were sourced from Al-Nibaie quarry, located northwest of Baghdad, Iraq. These aggregates were quantified and graded in accordance with AASHTO M 43 and ASSHTO T-27 [14, 15], with a maximum size of 4.75 mm for natural sand and 19 mm for crushed gravel. Figure 1 illustrates the gradation curves of both aggregates, while Table II summarizes their physical properties and sulfate content.

C. Water and Superplasticizing

Ordinary potable water was employed for concrete mixing and curing, complying with the requirements of Iraqi Specification No. 417/2001. The chloride content was 64.3 mg/L, enough below the specified limit of 200 mg/L. Additionally, the pH and sulfate content were measured at 7.1 and 114.3 mg/L, respectively, both of which are within the acceptable ranges (pH: 6.5-8.5; sulfate: < 200 mg/L).

There are many modern admixtures that have been developed for concrete production, but superplasticizers are recognized to be the most effective agents for decreasing the water-to-cement ratio, which is an important property for producing high-performance concrete. Therefore, in this study, the superplasticizer used was Sika (Visco-Crete)-171, which is reportedly good in achieving fast curing and a reduction in the water demand for the mixing of concrete [16].

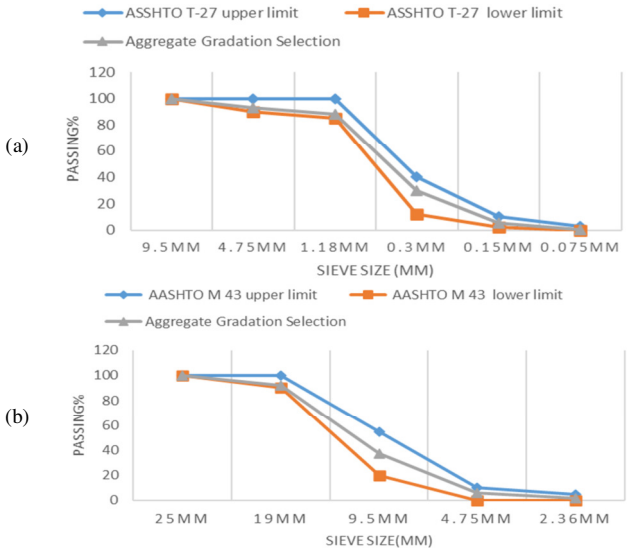

Fig. 1. The graduation of (a) natural sand and (b) crushed gravel.

TABLE II. PHYSICAL PARAMETERS AND SULFATE CONTENT OF AGGREGATES

Property	**Fine aggregate**	**ASTM C33**	**Coarse aggregate**	**ASTM C33**
Specific gravity	2.56	-	2.60	-
Absorption	1.22%	-	0.38	-
Sulfate content	0.15%	≤ 0.5%	0.05%	≤0.1%

D. Fibers

Two types of fibers were incorporated into the concrete mixes in three configurations: exclusively steel fibers, exclusively carbon fibers, and a hybrid combination of both steel and carbon fibers, as displayed in Figure 2. Their selection involved their compatibility with the concrete matrix and their ability to enhance the mechanical properties of the pavement. Detailed characteristics of these fibers are provided in Table III [17].

TABLE III. THE CHARACTERISTICS OF FIBERS

Property	**Steel fiber (KF-71/50-CH)**	**Carbon fiber (chopped strands)**
Density/specific gravity	7800 kg/m³	1.65-1.75 g/cm³
Tensile strength (MPa)	900-2200	3500-3700
Modulus of elasticity (GPa)	200	220-240
Average length (mm)	50	6
Nominal diameter (mm)	0.7	0.7
Aspect ratio	71	8.5

* Provided by the manufacturer

Six concrete mixes were prepared: a control mix without fiber, a single-fiber mix with 1% steel fiber, a single-fiber mix with 1% carbon fiber, and three hybrid mixes with a total fiber content of 1%, comprising 0.75% steel /0.25% carbon fiber, 0.25% steel /0.75% carbon fiber, and 0.5% steel /0.5% carbon fiber. Incorporating fibers necessitated adjustments in superplasticizer dosage to maintain workability, as the increased fiber surface area could disrupt the mix's homogeneity [18]. Table IV details the various mixtures, their fiber contents, and the corresponding superplasticizer dosages.

(a)

(b)

(c)

Fig. 2. (a) Steel fiber, (b) carbon fiber, and (c) hybrid fiber (steel and carbon).

TABLE IV. MIXTURES USED, FIBER, SUPERPLASTICIZING PERCENTAGES

Mix	Description	Superplasticizer
Con.	Control Mix	0.50%
SF1%	Concrete mix with adding 1% steel fiber (single mix)	0.60%
CF1%	Concrete mix with adding 1% carbon fiber (single mix)	0.65%
SF0.75 CF0.25	Concrete mix with adding 0.75% steel fiber and 0.25% carbon fiber (hybrid mix)	0.62%
SF0.25 CF0.75	Concrete mix with adding 0.25% steel fiber and 0.75% carbon fiber (hybrid mix)	0.64%
SF0.50 CF0.5	Concrete mix with adding 0.50% steel fiber and 0.50% carbon fiber (hybrid mix)	0.64%

III. MIX DESIGN, CASTING, CURING

The concrete mixture was designed according to ACI 211.1 [19] to achieve a target compressive strength of 30 MPa. The mix proportions per cubic meter were 360 kg of cement, 800 kg of fine aggregate, 994 kg of crushed gravel, and 117 kg of water. After a thorough mixing, the concrete was cast into molds and compacted to minimize entrapped air. The samples were de-molded after 24 hours and then cured in a water bath at 20 ± 2 °C for predetermined periods of 7, 28, and 90 days, ensuring proper hydration and strength development. This controlled curing process was critical for achieving the desired mechanical properties and durability for high-performance concrete pavements.

IV. MECHANICAL TESTS

A. Compressive Strength Test

To evaluate the compressive performance of concrete mixtures, three standard cubes (150 mm × 150 mm × 150 mm) were prepared for each mix following the BS1811-116 standard [20], with the average results having been recorded as the representative compressive strength for the corresponding mix. A standardized compression machine was utilized at a controlled rate of 0.14-0.34 MPa/sec. The tests were conducted at curing ages of 7, 28, and 90 days. Figure 3 presents the compressive strength test setup.

Fig. 3. Compressive strength test setup.

B. Flexural Strength Test

The flexural strength test was conducted in accordance with ASTM C78/C78M [21] to estimate the concrete's resistance to bending stresses using a point loading configuration, as evidenced in Figure 4.

Fig. 4. Flexural strength test.

Three replicate specimens were tested, and the average result was recorded as the modulus of rupture (f_r, in MPa), calculated using:

$$f_r = \frac{P \cdot L}{4 \cdot b \cdot d^2} \quad (1)$$

where P is the maximum applied load (N), L is the span length (mm), b is the average width of the specimen at the fracture (mm), and d is the average depth of the specimen at the fracture (mm).

C. Splitting Tensile Strength Test

For the splitting tensile strength test, cylindrical specimens with a diameter of 100 mm and a length of 200 mm were prepared according to ASTM C496/C496M [22]. The load was applied gradually at a controlled rate ranging from 1.2 N/(mm²·min) to 2.4 N/(mm²·min) to achieve uniform stress distribution without sudden impact. The splitting tensile strength was calculated by:

$$f_{ct} = \frac{2P}{\pi DL} \quad (2)$$

where f_{ct} is the splitting tensile strength (MPa), P is the maximum applied load (N), D is the diameter of the cylinder (mm), and L is the length of the cylinder (mm). Figure 5 illustrates the test setup of this procedure. The testing protocol provides a measure of the concrete's resistance to cracking and failure under tensile stress, which is essential for assessing the durability and service life of rigid pavements.

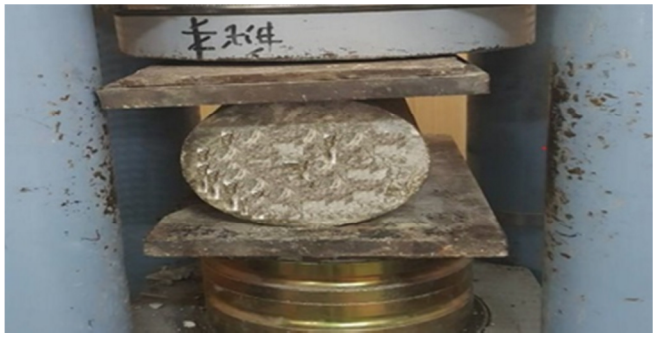

Fig. 5. Splitting tensile strength test.

V. FINITE ELEMENT MODELING

The concrete pavement evaluated using ABAQUS software consisted of three layers: a concrete slab, a granular subbase, and a subgrade layer. The dimensions for the concrete slab and granular subbase were determined based on AASHTO guidelines [23], while the subgrade thickness was assumed based on the premise that vertical stress dissolves after approximately 1.5 m from the pavement surface [24]. Tables V and VI summarize the physical properties assigned to each layer [30, 31].

The stress-strain behavior of the materials in compression and tension was defined using the Saenz model [25]. The support form pavement was being modeled, whereby the bottom surface of the subgrade is fully restrained in the U1, U2, and U3 directions to simulate the behavior of fixed boundary conditions and resist rigid body motion [26]. The interaction between concrete slab, subbase, and subgrade was defined through tie constraints assuring full bonding and displacement compatibility between the layers [27]. A mesh sensitivity analysis was carried out with mesh sizes of 200, 150, 100, 80, and 50 mm. The 50 mm mesh was found to provide the best compromise between accuracy and computational efficiency, consistent with the finite element modeling practices in pavement analysis in [28]. Furthermore, the dual tires of a truck axle were modeled as an equivalent rectangular contact area measuring 510 mm in width and 250 mm in length [28].

The material behavior of fiber-reinforced and non-fiber concrete was modeled using constitutive simulations reflecting their respective characteristics. The loading protocol was executed in two phases. First, a static displacement was applied until the maximum displacement corresponding to failure was reached. Second, the load was repeatedly applied with an incremental rate of 0.005, following procedures outlined in [26-29] The displacement response under repeated loading was then analyzed to assess the effect of fiber reinforcement on the pavement's structural performance.

Figure 6 presents the three-layer configuration of the concrete pavement model, and Table VII details the plasticity parameters employed for the subbase and subgrade layers [30, 31].

(a)

(b)

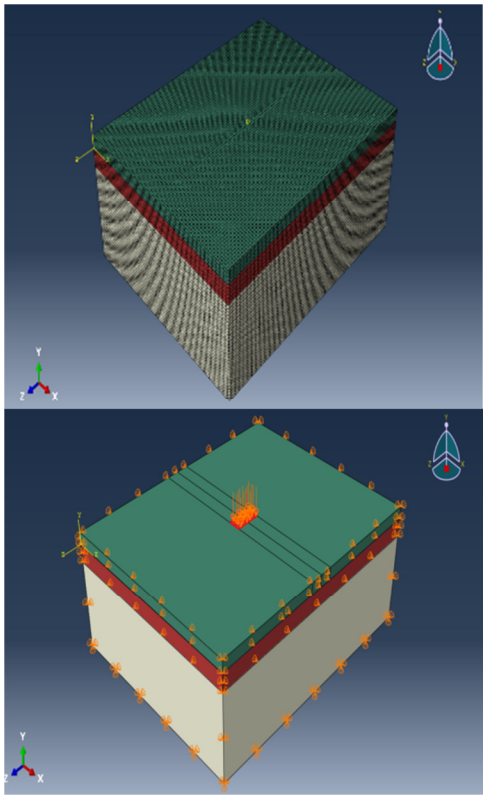

Fig. 6. (a) Mesh, (b) boundary conditions and loading configuration of the three-layer concrete pavement model.

TABLE V. PHYSICAL PROPERTIES OF THE MODEL [30-31]

Layers	Poisson ratio	Young modulus (MPa)	Density, (kg/m^3)	Width mm)	Length (mm)	Thickness (mm)
Concrete	0.2	Var.*	2400	4000	5000	200
Granular subbase	0.35	110	1850	4000	5000	300
Subgrade	0.35	10	1665	4000	5000	1500

* From this study

TABLE VI. CONCRETE DAMAGED PLASTICITY PARAMETERS USED IN ABAQUS

Dilation angle	Eccentricity	f_{b0}/f_{c0}	K (ratio)	Viscosity parameter
36°	0.1	1.16	0.667	1.00E-05

TABLE VII. PLASTICITY MODEL PARAMETERS [30-31]

Materials	Friction angle	Dilation angle	Cohesion yield stress (MPa)
Subbase	40°	10°	0.15
Subgrade	10°	0°	0.0436

VI. RESULTS AND DISCUSSION

A. Compressive Strength Test

All concrete mixtures exhibited a progressive increase in compressive strength over time, as presented in Figure 7 and Table VIII. The control mix recorded values of 24.4 MPa, 32.5 MPa, and 34.1 MPa at 7, 28, and 90 days, respectively, meeting the minimum strength limit proposed by ACI 325R.

At 28 days, the SF1% mix achieved a compressive strength of 35.4 MPa, representing an 8.9% improvement over the control mix. This enhancement can be attributed to the efficient load distribution and crack-bridging capabilities by the steel fibers, improving the overall material integrity. Similarly, the CF1% mix reached a strength of 34.7 MPa and a 6.8% increase over the control mix, suggesting that carbon fibers also contribute positively, though a slightly lesser extent than steel fibers. As for the hybrid mixes, intermediate performance was observed. Specifically, SF0.75CF0.25 attained 35.1 MPa (8.0% increase), SF0.25CF0.75 reached 34.6 MPa (7.0% increase), and SF0.5CF0.5 achieved 35.0 MPa (7.7% increase). Based on these findings, the SF1% mix is proposed as the most effective configuration for improving the compressive performance of concrete pavements.

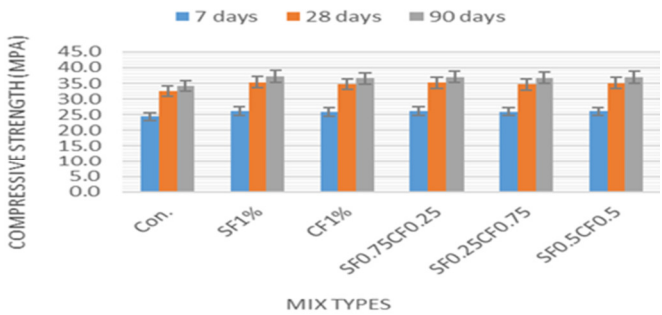

FIG. 7. Compressive strength of all mixes.

TABLE VIII. COMPRESSIVE STRENGTH RESULTS

Mix type	7 days (MPa)	28 days (MPa)	90 days (MPa)
Con.	24.4	32.5	34.1
SF1%	26.2	35.4	37.2
CF1%	25.9	34.7	36.6
SF0.75CF0.25	26.1	35.1	37.0
SF0.25CF0.75	26.0	34.6	36.7
SF0.5CF0.5	26.1	35.0	36.9

B. Flexural Strength Test

Figure 8 and Table IX present the evolution of flexural strength for both the control and fiber-reinforced mixes at 7, 28, and 90 days. The control mix achieved strengths of 3.160, 3.991, and 4.190 MPa, respectively. The SF1% mix demonstrated significant improvements, with flexural strengths of 5.239 MPa at 7 days, 6.804 MPa at 28 days, and 7.228 MPa at 90 days. This corresponds to a 72.5% increase over the control mix at 90 days. The CF1% also enhanced flexural strength, reaching 6.227 MPa at 90 days (a 48.6% improvement compared to the control mix). The hybrid mixes showed intermediate improvements, indicating synergistic effects when combining steel and carbon fibers. At 90 days, SF0.75CF0.25 reached 7.132 MPa (a 70.2% improvement), SF0.5CF0.5 recorded 6.788 MPa (62% higher than the control mix), and SF0.25CF0.75 attained 6.692 MPa (a 59.7% increase). These results confirm that fiber reinforcement, significantly enhances the flexural capacity of concrete, further improving crack resistance and extending pavement service life. Notably, the SF1% consistently achieved the highest flexural strength, being proposed as the most effective option among the evaluated mixes.

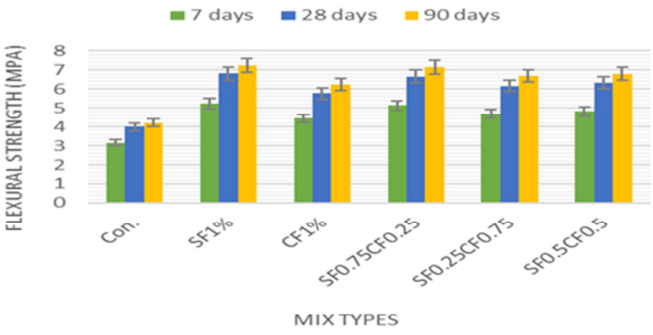

Fig. 8. Flexural strength of different mixes.

TABLE IX. FLEXURAL STRENGTH RESULTS

Mix type	7 days (MPa)	28 days (MPa)	90 days (MPa)
Con.	3.160	3.991	4.190
SF1%	5.239	6.804	7.228
CF1%	4.439	5.766	6.227
SF0.75CF0.25	5.119	6.656	7.132
SF0.25CF0.75	4.683	6.162	6.692
SF0.5CF0.5	4.803	6.305	6.788

C. Splitting Tensile Strength Test

Figure 9 and Table X present the splitting tensile strength results for both the control and fiber-reinforced mixes at 7, 28, and 90 days. The control mix exhibited a tensile strength of 2.736 MPa, 3.649 MPa, and 3.940 MPa, respectively. The 1% steel fiber mix (SF1%) demonstrated a marked improvement, achieving 4.466 MPa at 7 days, 6.155 MPa at 28 days, and 6.699 MPa at 90 days, representing a 70% increase over the control mix at 90 days. The 1% carbon fiber mix (CF1%) also exhibited notable gains in splitting tensile strength, with values of 3.760 MPa, 5.155 MPa, and 5.733 MPa at 7, 28, and 90 days, respectively, corresponding to a 45.5% improvement compared to the control mix at 90 days.

Meanwhile, the hybrid mixes showed intermediate enhancements, reflecting the combined benefits of steel and carbon fibers. At 90 days, SF0.75CF0.25 reached 6.612 MPa (a 67.8% increase), SF0.25CF0.75 recorded 6.151 MPa (a 56% rise), and SF0.5CF0.5 achieved 6.234 MPa (about a 58% improvement).These findings indicated that fiber reinforcement significantly enhanced the tensile capacity of concrete, improving resistance to cracking and extending the potential service life of rigid pavements. Among the evaluated mixes, the 1% steel fiber mix consistently provided the highest splitting tensile strengths, underscoring its effectiveness in resisting tensile stresses.

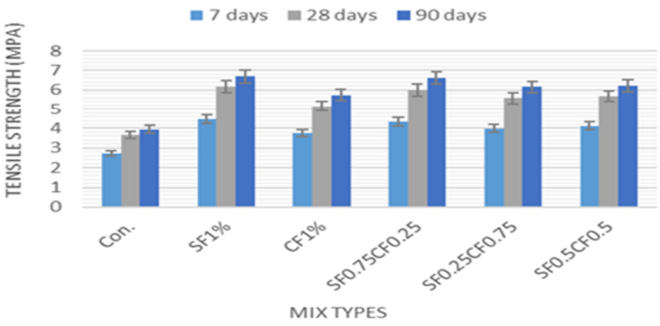

Fig. 9. Splitting tensile strength of different mixes

TABLE X. SPLITTING TENSILE STRENGTH RESULTS

Mix type	7 days (MPa)	28 days (MPa)	90 days (MPa)
Con.	2.736	3.649	3.940
SF1%	4.466	6.155	6.699
CF1%	3.760	5.155	5.733
SF0.75CF0.25	4.326	5.995	6.612
SF0.25CF0.75	3.984	5.575	6.151
SF0.5CF0.5	4.132	5.677	6.234

D. Finite Element Modeling

In the initial phase of the analysis, the concrete pavement model was subjected to a static displacement to determine the maximum load corresponding to failure, as indicated by the peak deformation. Once these load values were identified, a dynamic loading phase was initiated during which the load was incrementally applied at a rate of 0.05 over a duration of 39 seconds until each model reached its maximum displacement.

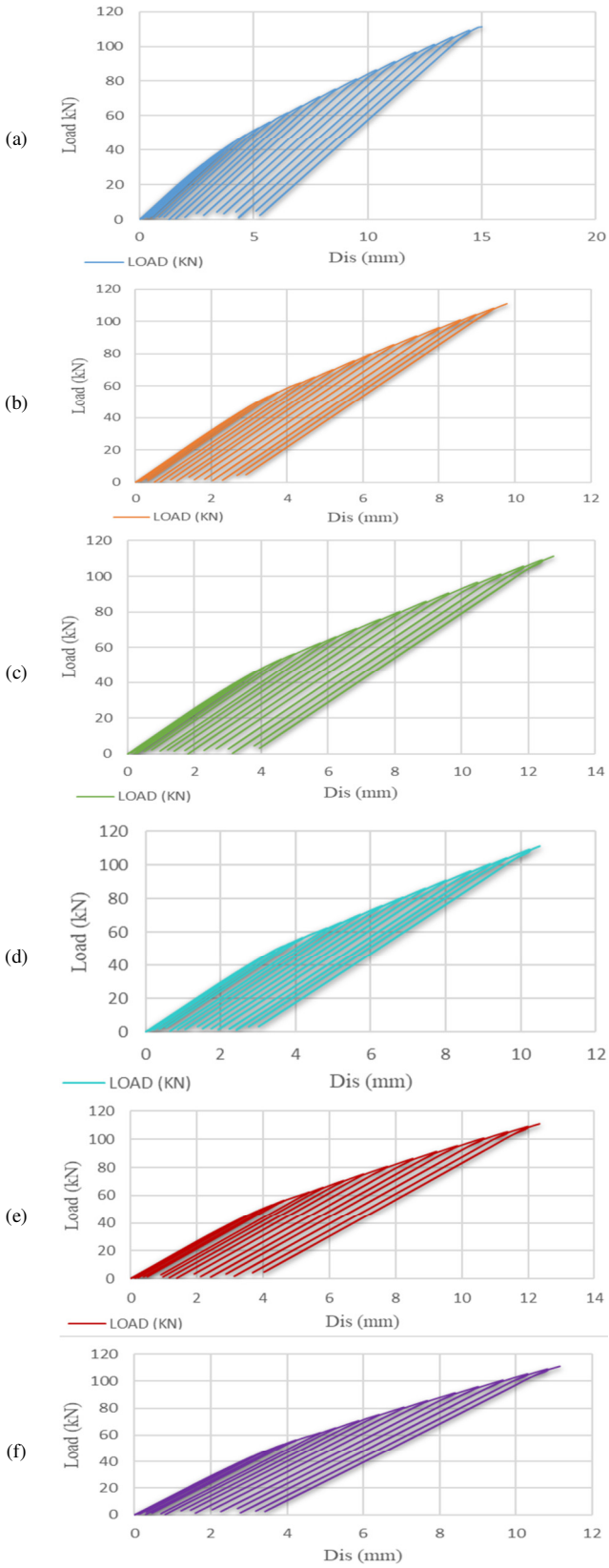

Fig. 10. Displacement results of the model under repeated loading (a) Con., (b) SF1%, (c) CF1%, (d) SF0.75CF0.25, (e) SF0.25CF0.75, (f) SF0.5CF0.5.

The measured displacement represents the cumulative deformation across all three pavement layers: the concrete slab, granular subbase, and subgrade. Figure 10 depicts the overall finite element model subjected to repeated loading, while Figures 11 and 12 illustrate the displacement outcomes under static and repeated loading, respectively. The analysis reveals that fiber reinforcement substantially mitigates pavement deformation. Among the single-fiber configurations, the 1% steel fiber mix exhibited the most pronounced reduction in displacement, achieving a 35% decrease relative to the control mix. In contrast, the 1% carbon fiber mix resulted in a more modest reduction of about 15%. Hybrid mixes, combining steel and carbon fibers in various proportions, produced intermediate improvements, with a reduction displacement of 30% for the SF0.75CF0.25 mix, a 18% reduction for the SF0.25CF0.75 mix, and a 23% decrease for the SF0.5CF0.5 mix.

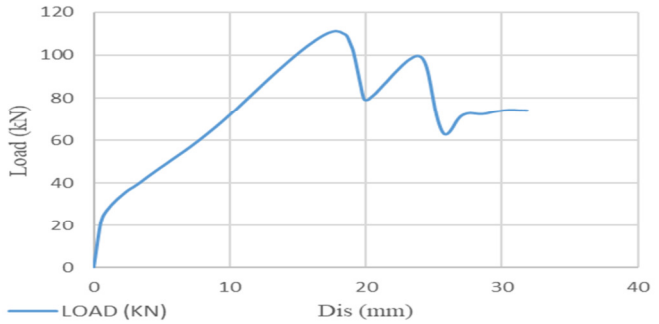

Fig. 11. The result of applying static displacement.

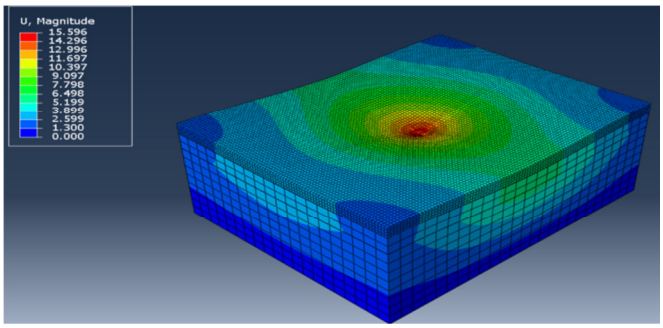

Fig. 12. Finite element model subjected to repeated loading.

Regression analysis was then applied to the displacement data to estimate pavement deformation under a standardized load of 50 kN. The corresponding regression equations and R^2 values (ranging from 0.90 to 0.91) are presented in Table XI, and a comparison of the displacement values between all mixes is illustrated in Figure 13. Under 50 kN load, the control mix exhibited a displacement of 6.42 mm, while the 1% steel fiber mix displayed a reduced value of 4.16 mm. Additionally, the 1% carbon fiber mix and the hybrid mixes yielded displacement values between 4.51 mm and 5.43 mm. Collectively, these finite element modeling results confirm that fiber reinforcement, particularly with steel fibers, significantly enhances the deformation resistance of concrete pavements. This finding aligns with previous research demonstrating the ability of steel fibers to control crack propagation and improve post-cracking stiffness under load [31, 32]. By integrating advanced numerical simulations with empirical data, this study provides a robust framework for understanding the structural benefits of fiber incorporation, thereby contributing to the development of more durable and resilient infrastructure.

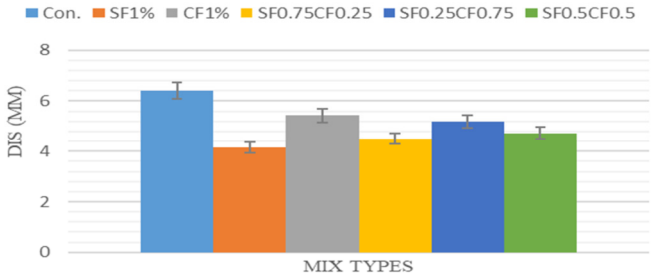

Fig. 13. Displacement comparison for various combinations.

TABLE XI. REGRESSION EQUATIONS AND DISPLACEMENTS UNDER 50 KN LOAD

Mix	Regression equation	R^2	Load (kN)	Displacement (mm)
Con.	y =7.4964x + 1.7985	0.91	50	6.42
SF1%	y =11.437x + 2.4129	0.90	50	4.16
CF1%	y =8.6458x + 3.0494	0.91	50	5.43
SF0.75CF0.25	y =10.607x + 2.1035	0.91	50	4.51
SF0.25CF0.75	y =8.8873x + 3.7407	0.90	50	5.20
SF0.5CF0.5	y =9.9089x + 3.0893	0.90	50	4.73

VII. CONCLUSION

This study presents an integrated experimental and numerical investigation into the mechanical and structural performance of concrete pavements reinforced with steel, carbon, and hybrid fibers. Laboratory testing assessed compressive, flexural, and splitting tensile strengths at 7, 28, and 90 days while Finite Element Analysis (FEA) under repeated loading provided insights into structural behavior. Based on the findings, the following conclusions are obtained:

- The application of fiber reinforcement significantly enhanced the mechanical performance of concrete. Among all fiber types, the 1% steel fiber (SF1%) exhibited the greatest improvement compared to carbon fibers and hybrid combinations. At 90 days, the 1% steel fiber mix increased compressive strength by 9.1% (37.2 MPa vs. 34.1 MPa), flexural strength by 72.5% (7.228 MPa vs. 4.190 MPa), and splitting tensile strength by 70% (6.699 MPa vs. 3.940 MPa).
- Significant improvements were observed in both flexural and splitting tensile strengths, attributable to the fibers' effective crack-arresting properties. The SF1% mix demonstrated a 72.5% increase in flexural strength and a 70% enhancement in splitting tensile strength compared to the control mix. Hybrid configurations delivered intermediate benefits, with flexural strength improvements ranging from 59.7% to 70.2% and splitting tensile strength enhancements between 56% and 67.8%.

- Finite element modeling further corroborated the experimental results by demonstrating a substantial reduction in pavement displacement under repeated loading. Under a 50 kN load, the control mix exhibited a displacement of 6.42 mm, whereas the SF1% mix reduced this displacement to 4.16 mm, (approximately 35%). Hybrid mixes showed displacement values ranging from 4.51 mm to 5.43 mm, indicating a balanced improvement relative to single-fiber systems.

Overall, the integration of fiber reinforcement not only improves the mechanical properties of concrete, but also enhances its structural performance under dynamic loads. The numerical findings strongly suggest that fiber-reinforced concrete, particularly with 1% steel fiber, is a promising strategy for increasing durability and extending the service life of rigid pavements, thereby contributing to more resilient and sustainable infrastructure.

REFERENCES

[1] M. H. Dawood, A. F. Izzet, and B. H. Khudair, "Performance of concrete thrust block at several burial conditions under the influence of thrust forces generated in the water distribution networks," *Journal of the Mechanical Behavior of Materials*, vol. 31, no. 1, pp. 473–483, Jan. 2022, https://doi.org/10.1515/jmbm-2022-0048.

[2] M. V. Mohod and K. N. Kadam, "A comparative study on rigid and flexible pavement: A review," *IOSR Journal of Mechanical and Civil Engineering (IOSR-JMCE)*, vol. 13, no. 3, pp. 84–88, 2016.

[3] S.-J. Jang *et al.*, "Effect of Contents, Tensile Strengths and Aspect Ratios of Hooked-End Steel Fibers (SFs) on Compressive and Flexural Performance of Normal Strength Concrete," *International Journal of Concrete Structures and Materials*, vol. 17, no. 1, Aug. 2023, Art. no. 46, https://doi.org/10.1186/s40069-023-00611-6.

[4] A. A. E. Elzokra, A. A. Houri, A. Habib, M. Habib, and A. B. Malkawi, "Shrinkage Behavior of Conventional and Nonconventional Concrete: A Review," *Civil Engineering Journal*, vol. 6, no. 9, pp. 1839–1851, Sep. 2020, https://doi.org/10.28991/cej-2020-03091586.

[5] M. Anas, M. Khan, H. Bilal, S. Jadoon, and M. N. Khan, "Fiber Reinforced Concrete: A Review," in *the 12th International Civil Engineering Conference (ICEC-2022)*, Karachi, Pakistan, May 2022, https://doi.org/10.3390/engproc2022022003.

[6] H. Z. Hassan and N. M. Saeed, "Fiber reinforced concrete: a state of the art," *Discover Materials*, vol. 4, no. 1, Dec. 2024, Art. no. 101, https://doi.org/10.1007/s43939-024-00171-w.

[7] M. B. Khan, M. Houda, N. S. Zada, M. Imran, and O. Benjeddou, "Hybrid effect of basalt fibers and carbon fibers on concrete mechanical and environmental properties," *Results in Engineering*, vol. 25, Mar. 2025, Art. no. 103780, https://doi.org/10.1016/j.rineng.2024.103780.

[8] P. B. Bhavish Bhat, T. M. Swaroop, K. Jayanth, and B. O. Naveen, "Experimental studies and non-linear finite element analysis of flexural behavior of steel fibre-reinforced concrete under monotonic and repeated cyclic loading," *Discover Civil Engineering*, vol. 1, no. 1, Aug. 2024, Art. no. 61, https://doi.org/10.1007/s44290-024-00066-y.

[9] G. A. Almashhadani and M. H. Al-Sherrawi, "Effect Change Concrete Slab Layer Thickness on Rigid Pavement," *Engineering, Technology & Applied Science Research*, vol. 12, no. 6, pp. 9661–9664, Dec. 2022, https://doi.org/10.48084/etasr.5283.

[10] N. K. Singh and B. Rai, "A Review of Fiber Synergy in Hybrid Fiber Reinforced Concrete," *Journal of Applied Engineering Sciences*, vol. 8, no. 2, pp. 41–50, Dec. 2018, https://doi.org/10.2478/jaes-2018-0017.

[11] B. Ali, L. A. Qureshi, and S. U. Khan, "Flexural behavior of glass fiber-reinforced recycled aggregate concrete and its impact on the cost and carbon footprint of concrete pavement," *Construction and Building Materials*, vol. 262, Nov. 2020, Art. no. 120820, https://doi.org/10.1016/j.conbuildmat.2020.120820.

[12] Z. R. Aljazaeri and Z. Al-Jaberi, "Numerical Study on Flexural Behavior of Concrete Beams Strengthened with Fiber Reinforced Cementitious Matrix Considering Different Concrete Compressive Strength and Steel Reinforcement Ratio," *International Journal of Engineering*, vol. 34, no. 4, 2021, https://doi.org/10.5829/ije.2021.34.04a.05.

[13] *Standard Specification for Portland Cement*, ASTM C150/C150M, 2022.

[14] *Standard Specification for Sizes of Aggregate for Road and Bidge Construction*, AASHTO M 43, 2005.

[15] *Standard Method of Test for Sieve Analysis of Fine and Coarse Aggregates*, AASHTO T 27, 1993.

[16] Sika Group, "Sika® ViscoCrete®-171 Precast: Product Data Sheet," Dec. 2022. [Online]. Available: https://irq.sika.com/dms/getdocument.get/0c9d59db-bc47-4dd1-8e22-744578e38802/sika-viscocrete-171precast.pdf.

[17] "Products." Haining ANJIE Composite Materials. https://www.anjiezj.com/products.

[18] "State-of-the Art Report on fiber reinforced concrete," American Concrete Institute, ACI 544.1 R-96, 1996.

[19] "Standard Practice for Selecting Proportions for Normal, Heavyweight, and Mass Concrete," American Concrete Institute, ACI 211.1-91, 1991.

[20] *Method for determination of compressive strength of concrete cubes*, BS 1881-116, 1983.

[21] *Standard Test Method for Flexural Strength of Concrete (Using Simple Beam with Third-Point Loading)*, ASTM C78/C78M, 2022.

[22] Standard test method for splitting tensile strength of cylindrical concrete specimens, ASTM C496/C496M, 2017.

[23] *AASHTO Guide for Design of Pavement Structures*. WA, USA: American Association of State Highway and Transportation Officials.

[24] H.-G. Kwak and F. Filippou, "Finite element analysis of reinforced concrete structures under monotonic loads," University of California, Berkeley, CA, USA, UCB/SEMM-90, 1990.

[25] L. P. Saenz, " Discussion of equation for the stress-strain curve of concrete," *ACI Journal Proceedings*, vol. 61, no. 9, pp. 1229–1235, 1964.

[26] H. M. Shakir, A. A. Al-Azzawi, and A. F. Al-Tameemi, "Nonlinear Finite Element Analysis of Fiber Reinforced Concrete Pavement under Dynamic Loading," *Journal of Engineering*, vol. 28, no. 2, pp. 81–98, Feb. 2022, https://doi.org/10.31026/j.eng.2022.02.06.

[27] A. Jagadeesh, W. A. A. S. Premarathna, A. Kumar, C. Kasbergen, and S. Erkens, "Finite element modelling of jointed plain concrete pavements under rolling forklift tire," *Engineering Structures*, vol. 328, Apr. 2025, Art. no. 119705, https://doi.org/10.1016/j.engstruct.2025.119705.

[28] Y. H. Huang, *Pavement Analysis Design*, 2nd ed. Upper Saddle River, NJ, USA: Pearson/Prentice Hall, 2004.

[29] M. H. Dawood, A. F. Izzet, and B. H. Khudair, "Optimal Bedding Selection with the Specific Soil Type According to the Thrust Forces Generated in the Water Distribution Networks Using the Restraining Joint System," in *Proceedings of 3ICGE-Iraq 2022*, Singapore, 2023, pp. 38–51, https://doi.org/10.1007/978-981-19-7358-1_5.

[30] Z. Yin, K. M. Ndiema, R. L. Lekalpure, and C. K. Kiptum, "Numerical Study of Geotextile-Reinforced Flexible Pavement Overlying Low-Strength Subgrade," *Applied Sciences*, vol. 12, no. 20, Jan. 2022, Art. no. 10325, https://doi.org/10.3390/app122010325.

[31] A. E. A. El-Maaty, "Improving Rutting Resistance of Flexible Pavement Using Geosynthetics," *Open Access Library Journal*, vol. 03, no. 05, 2016, Art. no, 69304, https://doi.org/10.4236/oalib.1102655.

[32] M. Hamrat, B. Boulekbache, T. Tahenni, M. Chemrouk, and S. Amziane, "Experimental study of deflection of steel fibre reinforced concrete beams: comparison of different design codes," *European Journal of Environmental and Civil Engineering*, vol. 26, no. 6, pp. 2057–2073, Apr. 2022, https://doi.org/10.1080/19648189.2020.1749941.